

## van der Waals and Casimir interactions between atoms and carbon nanotubes

This article has been downloaded from IOPscience. Please scroll down to see the full text article.

2008 J. Phys. A: Math. Theor. 41 164012

(<http://iopscience.iop.org/1751-8121/41/16/164012>)

View [the table of contents for this issue](#), or go to the [journal homepage](#) for more

### Download details:

IP Address: 171.66.16.148

The article was downloaded on 03/06/2010 at 06:44

Please note that [terms and conditions apply](#).

# van der Waals and Casimir interactions between atoms and carbon nanotubes

G L Klimchitskaya<sup>1,2</sup>, E V Blagov<sup>3</sup> and V M Mostepanenko<sup>1,3</sup>

<sup>1</sup> Center of Theoretical Studies and Institute for Theoretical Physics, Leipzig University, D-04009 Leipzig, Germany

<sup>2</sup> North-West Technical University, Millionnaya St 5, St Petersburg 191065, Russia

<sup>3</sup> Noncommercial Partnership 'Scientific Instruments', Tverskaya St 11, Moscow 103905, Russia

Received 3 November 2007, in final form 30 January 2008

Published 9 April 2008

Online at [stacks.iop.org/JPhysA/41/164012](http://stacks.iop.org/JPhysA/41/164012)

## Abstract

The van der Waals and Casimir interactions of a hydrogen atom (molecule) with a single-walled and a multi-walled carbon nanotubes are compared. It is shown that the macroscopic concept of graphite dielectric permittivity is already applicable for nanotubes with only two or three walls. The absorption of hydrogen atoms by a nanotube at separations below 1 nm is considered. The lateral force due to exchange repulsion moves the atom to a position above the cell center, where it is absorbed by the nanotube because the repulsive force cannot balance the van der Waals attraction.

PACS numbers: 73.22.-f, 34.50.Dy, 12.20.Ds

## 1. Introduction

Considerable recent attention has been focused on applications of the van der Waals and Casimir forces in nanotechnology. When the characteristic sizes of microdevices shrink below a micrometer, the collective quantum phenomena caused by the existence of zero-point oscillations of the electromagnetic field come into play. At separations below 100 nm the role of physical phenomena originating from vacuum oscillations (primarily of the van der Waals and Casimir forces) can match the role of characteristic electric force and may even become dominant. This was first stressed long ago in [1] and was commonly accepted in the beginning of the third millennium. By then several experiments on measurement of the Casimir force between metallic surfaces had already been performed [2]. This laid the groundwork for the application of dispersion forces (which is a generic name for the van der Waals and Casimir force) in nanomechanical devices [3–5], noncontact atomic friction [6–10], carbon nanostructures [12–14] and related subjects. Thereafter, the precision of measurements of the Casimir force was significantly increased [15] and different methods to control the force magnitude were elaborated [16] opening possible applications to nanotweezers, nanoscale actuators and other nanomachines.

Dispersion interaction is also of much importance for the understanding of absorption phenomena of atoms and molecules by nanostructures. This subject is currently topical in connection with the problem of hydrogen storage in carbon nanotubes. Until recently it was studied using the phenomenological density-functional theory (see, e.g. [11, 12, 14]). In [17, 18] the Lifshitz theory of the van der Waals and Casimir force [19] was applied for the cases of an atom (molecule) interacting with a plane surface of a graphite plate or multiwall carbon nanotube. This was achieved by using a classical model of the frequency-dependent dielectric permittivities of a uniaxial crystal and proximity force approximation [20].

Some properties of the monoatomic sheet of C atoms (graphene) admit a simplified model description in terms of the two-dimensional free electron gas. In doing so the graphene sheet is characterized by some typical wave number  $K$  determined by the parameters of the hexagonal structure of graphite. In [21] the interaction of the electromagnetic oscillations with such a sheet was considered and the reflection coefficients were found. In [22] the Lifshitz-type formula was obtained for the van der Waals and Casimir interaction between the two parallel plasma sheets. Using this model in [23] the interaction between graphene and a material plate, graphene and an atom or a molecule, and between a single-walled carbon nanotube and a material plate was also described by means of the Lifshitz-type formulae. Finally, in [24] the Lifshitz-type formula was obtained for the van der Waals and Casimir interaction between an atom (molecule) and a single-walled carbon nanotube. All above mentioned results are applicable if the separation distances are sufficiently large (typically larger than 1 nm).

In this paper, we compare the van der Waals interactions of a hydrogen atom (molecule) with a single-walled and a multi-walled carbon nanotube. The former is approximately modeled as a cylindrical plasma sheet, whereas the latter as a cylindrical shell of finite thickness characterized by graphite dielectric permittivities for the ordinary and extraordinary rays. We arrive at the conclusion that the macroscopic concept of dielectric permittivity is already applicable for nanotubes containing only two or three walls (section 2). We also consider the interaction of atoms or molecules with carbon nanotubes at separations below 1 nm where the Lifshitz-type formulae obtained in [22–24] are not applicable. Using the method of phenomenological potentials and disregarding the role of chemical forces, we find that at separations below 1 nm the exchange repulsion gives rise to the lateral force that moves hydrogen atoms toward the cell center. In the position above a cell center, the repulsive force cannot balance the van der Waals attraction. As a result, the atom penetrates inside the nanotube (section 3). This effect is analogous to the breaks of constant force surfaces that arise when scanning the monoatomic tip of an atomic force microscope above a closely packed lattice in contact mode [25, 26]. The discussion of the obtained results and conclusions are contained in section 4.

## 2. Comparison of atom–nanotube interaction in the cases of multiwalled and single-walled nanotubes

The free energy and force between an atom (molecule) and a multi-walled or single-walled carbon nanotube separated by a distance  $a$  can be represented in the form

$$\mathcal{F}(a, T) = -\frac{C_3(a, T)}{a^3}, \quad F(a, T) = -\frac{C_F(a, T)}{a^4}. \quad (1)$$

Here,  $T$  is the temperature of graphite which is supposed to be in thermal equilibrium with the surroundings. The coefficients  $C_3(a, T)$  and  $C_F(a, T)$  are defined in such a way that at short separations equation (1) reproduces the nonrelativistic van der Waals interaction (in this limit  $C_3$  and  $C_F$  do not depend on separation and temperature and it holds  $C_F = 3C_3$ ).

The Lifshitz-type formula for the coefficient  $C_3(a, T)$  was obtained in [17, 24] by using the proximity force approximation [20, 27]

$$C_3(a, T) = \frac{k_B T}{8} \sqrt{\frac{R}{R+a}} \left\{ \frac{4R+3a}{2(R+a)} \alpha(0) + \sum_{l=1}^{\infty} \alpha(i\zeta_l \omega_c) \int_{\zeta_l}^{\infty} dy y e^{-y} \left[ y - \frac{a}{2(R+a)} \right] \right. \\ \left. \times \left[ 2r_{\text{TM}}(i\zeta_l, y) + \frac{\zeta_l^2}{y^2} (r_{\text{TE}}(i\zeta_l, y) - r_{\text{TM}}(i\zeta_l, y)) \right] \right\}. \quad (2)$$

Here,  $R$  is the nanotube radius,  $\alpha(\omega)$  is the dynamic polarizability of an atom or a molecule,  $k_B$  is the Boltzmann constant and the dimensionless Matsubara frequencies  $\zeta_l$  are connected with the dimensional ones by the equalities

$$\zeta_l = \frac{\xi_l}{\omega_c}, \quad \xi_l = 2\pi \frac{k_B T}{\hbar} l, \quad \omega_c = \frac{c}{2a}, \quad l = 0, 1, 2, \dots \quad (3)$$

In our model description, the reflection coefficients for the two independent polarizations of the electromagnetic field,  $r_{\text{TM}}$  and  $r_{\text{TE}}$ , have different forms in the cases of multi-walled and single-walled carbon nanotubes. For multiwall nanotubes, they are expressed in terms of two dissimilar dielectric permittivities of graphite,  $\varepsilon_x(\omega) = \varepsilon_y(\omega)$  and  $\varepsilon_z(\omega)$ , where the crystal optical axis  $z$  is perpendicular to a cylindrical surface

$$r_{\text{TM}}^{\text{mw}}(i\zeta_l, y) = \frac{\varepsilon_{xl}\varepsilon_{zl}y^2 - f_z^2}{\varepsilon_{xl}\varepsilon_{zl}y^2 + f_z^2 + 2\sqrt{\varepsilon_{xl}\varepsilon_{zl}}yf_z \coth[f_z d/(2a)]}, \quad (4) \\ r_{\text{TE}}^{\text{mw}}(i\zeta_l, y) = \frac{f_x^2 - y^2}{f_x^2 + y^2 + 2yf_x \coth[f_x d/(2a)]}.$$

Here, the thickness of a nanotube is  $d = 3.4(N - 1) \text{ \AA}$ , where  $N$  is the number of walls, and the following notations are introduced:

$$\varepsilon_{xl} = \varepsilon_x(i\zeta_l \omega_c), \quad \varepsilon_{zl} = \varepsilon_z(i\zeta_l \omega_c), \quad (5) \\ f_z^2 = y^2 + \zeta_l^2(\varepsilon_{zl} - 1), \quad f_x^2 = y^2 + \zeta_l^2(\varepsilon_{xl} - 1).$$

The dielectric permittivities of graphite along the imaginary frequency axis are calculated in [17] on the basis of tabulated optical data from [28].

For single-walled nanotubes, we use the simplified model description by means of a cylindrical plasma sheet. Then the reflection coefficients are expressed in terms of the wave number of the sheet,  $K$ , which is determined by the density  $n$  of  $\pi$  electrons. Bearing in mind that there are two  $\pi$  electrons per one hexagonal cell with a side length  $r_0 = 1.421 \text{ \AA}$ , we arrive at

$$K = 2\pi \frac{ne^2}{mc^2} = 6.75 \times 10^5 \text{ m}^{-1}, \quad n = \frac{4}{3\sqrt{3}r_0^2}, \quad (6)$$

where  $e$  and  $m$  are the electron charge and mass, respectively. The resulting coefficients are

$$r_{\text{TM}}^{\text{sw}}(i\zeta_l, y) = \frac{2yaK}{2yaK + \zeta_l^2}, \quad r_{\text{TE}}^{\text{sw}}(i\zeta_l, y) = \frac{2aK}{2aK + y}. \quad (7)$$

The Lifshitz-type formula for the coefficient  $C_F(a, T)$  in (1) can be presented using the same notations [17, 24]. We emphasize that within the considered models equation (1) with the coefficients  $C_3$  and  $C_F$  is applicable at both short and large separations, i.e. both in nonrelativistic and relativistic regimes, and also in the transition region between the two regimes. We, however, consider  $a > 1 \text{ nm}$  because at shorter separations the atomic structure of nanotube wall and also other forces of different physical nature in addition to dispersion interaction should be taken into account. In the framework of used models, the error introduced

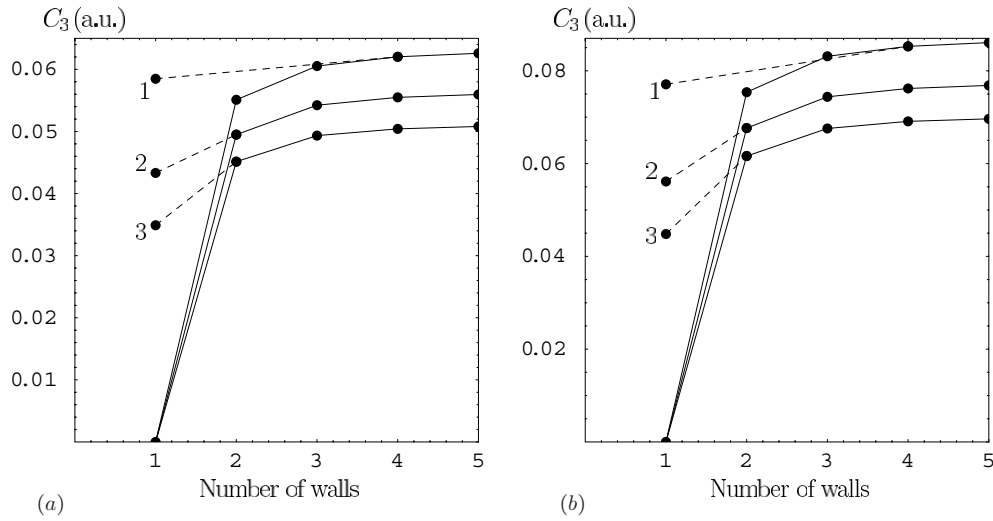


**Figure 1.** The van der Waals coefficient as a function of the number of walls for hydrogen atom (a) and molecule (b) interacting with the multi-walled carbon nanotube (solid dots connected with solid lines) and with the single-walled carbon nanotube (solid dots 1, 2 and 3) both of  $R = 5$  nm radius spaced at 1, 2, and 3 nm from the atom (a) or molecule (b). The thicknesses of multi-walled nanotubes with 2, 3, 4 and 5 walls are 0.34, 0.68, 1.02 and 1.36 nm, respectively.

from the application of the proximity force approximation is less than 1% within the separation region from 0 to  $R/2$  [27]. It is notable also that the above models do not take into account nanotube chirality. This can be included by using the optical data for nanotube complex index of refraction. We would like to underline that the used models, especially the model of a cylindrical plasma sheet in application to single-walled carbon nanotubes, do not claim a complete description of all nanotube properties. Specifically, it remains unclear if it is possible to describe nanotubes with surfaces like metals and like semiconductors by varying only one parameter  $K$  in the reflection coefficients (7).

To perform computations using above equations in the case of hydrogen atoms and molecules, one needs the explicit expressions for the atomic and molecular dynamic polarizabilities. As was shown in [17, 29], the dynamic polarizability can be represented with sufficient precision using the single-oscillator model

$$\alpha_a(i\xi_l) = \frac{g_a}{\omega_a^2 + \xi_l^2}, \quad \alpha_m(i\xi_l) = \frac{g_m}{\omega_m^2 + \xi_l^2} \quad (8)$$

for hydrogen atom and molecule, respectively. Here,  $\alpha_a(0) = 4.50$  au,  $\omega_a = 11.65$  eV,  $\alpha_m(0) = 5.439$  au,  $\omega_m = 14.09$  eV.

We have performed computations of the van der Waals free energy of hydrogen atoms and molecules and multi-walled and single-walled carbon nanotubes modeled as discussed above. For multi-walled nanotubes, equations (1), (2), (4), (8) were used. For single-walled nanotubes equation (4) was replaced with (7). The computational results for the coefficient  $C_3$  as a function of the number of walls are presented as solid dots in figure 1(a) (hydrogen atom) and in figure 1(b) (hydrogen molecule) for nanotubes with  $R = 5$  nm. In both cases the solid dots connected with a solid line are related to a multi-walled nanotube and the solid dots marked by 1, 2, and 3 are related to a single-walled nanotube for separation distances of  $a = 1, 2$  and 3 nm, respectively. For a ‘multi-walled’ nanotube with only one wall  $C_3 = 0$ , as

expected, because in this case nanotube thickness  $d = 0$  and hence the reflection coefficients (4) vanish. As is seen in figures 1(a) and (b), the magnitudes of the van der Waals coefficients  $C_3$  for a multiwalled nanotube with two walls at a separations of 2 or 3 nm from an atom or a molecule are in correct relation to the magnitudes computed for a single-walled nanotube (solid dots marked 2 and 3). Thus, the macroscopic concept of graphite dielectric permittivity is already applicable for nanotubes with only two or three walls provided the separation distance to an atom or a molecule is larger than 2 nm. For nanotubes with three walls the same holds for separations of 1 nm between an atom or a molecule and a nanotube. These results are expected because it is known that surface corrections to local fields in ordinary crystals generally become negligible already in the third or fourth lattice plane. Similar results but with other numerical values are also valid for the force coefficient  $C_F$ . To give an example, for nanotubes of  $R = 5$  nm radius at  $a = 1$  nm from a hydrogen atom  $C_3 = 0.0585$  au but  $C_F = 0.197$  au. At the same separation but for nanotubes of  $R = 2$  nm radius,  $C_3 = 0.0503$  au and  $C_F = 0.175$  au.

### 3. Absorption of hydrogen atoms by carbon nanotubes

The above formalism based on the Lifshitz-type formulae permits to calculate the attractive van der Waals and Casimir force acting between both multi-walled and single-walled carbon nanotubes and hydrogen atoms or molecules down to 1 nm separation distance using the simplified models described above. However, at shorter separations the atomic structure of nanotube and some other physical interactions in addition to dispersion forces should be taken into account. Because of this, complete calculation of absorption power of carbon nanotubes requires a detailed investigation of the microscopic interaction mechanisms including chemical forces and short-range exchange forces. The comparative role of different forces in absorption process has not been yet investigated. Below we consider the role of dispersion and exchange forces at separations less than 1 nm. We argue that the combined action of the interatomic attractive van der Waals force and of the repulsive exchange force, taken into account using a simple model, leads to the absorption of hydrogen atom by a nanotube. The investigation of the role of chemical forces is an interesting problem to be solved in future.

The exchange repulsion between C and H atoms at a separation  $r$  apart can be approximately described by means of the phenomenological potential  $U_{\text{rep}}(r) = \alpha/r^{12}$  [30], where  $\alpha$  is some coefficient. Papers [25, 26] investigated the scanning of the monoatomic tip of an atomic force microscope along the constant force surface above the closely packed crystal lattice in contact mode. It was supposed that the repulsive potential  $U_{\text{rep}}(r)$  is the single factor to be taken into account. As was shown in [25, 26], if the initial height of the tip  $h$  satisfies the condition  $h/r_0 > 0.61$  (here,  $r_0$  is the equilibrium interatomic distance in the lattice), the constant force surface under consideration is continuous. If, however, the initial height is sufficiently small ( $h/r_0 \leq 0.61$ ), the constant force surfaces have breaks above the regions between crystal atoms. For graphite lattice the atom in the center of a hexagonal cell is missing which only increases the areas of the breaks.

Let us consider now the hexagonal lattice shown in figure 2(a) with a hydrogen atom at a height  $h$  above it in the positions between points A and B (the lattice parameter is  $r_0$ ). There is the lateral force acting on an atom at a height  $h$  directed to a cell center. This can be seen in the following way. Let us consider the total repulsive energy due to interaction with a potential  $U_{\text{rep}}$  with all nearest C atoms with coordinates  $(x_i, y_i, 0)$ , e.g. with four atoms in the position A and six atoms in the position B (the first coordinative sphere). This energy is given by

$$E_{\text{rep}}(x, h) = \sum_i \frac{\alpha}{[(x - x_i)^2 + y_i^2 + h^2]^6}, \quad (9)$$

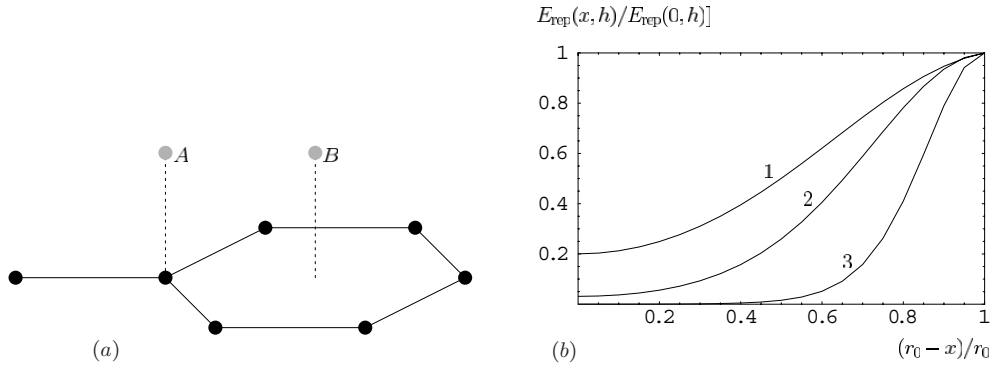


**Figure 2.** (a) Hydrogen atoms in the positions A and B at a height  $h$  above the hexagonal lattice of C atoms. (b) The relative energy of exchange repulsive interaction between the hydrogen atom at a height  $h$  above the hexagonal lattice of C atoms and neighboring C atoms as a function of  $(r_0 - x)/r_0$ . Here  $x$  is the lateral displacement from the C atom below a point A to the center of the cell.

where  $x = 0$  in the position A and  $x = r_0$  in the position B. In figure 2(b) we plot the ratio  $E_{\text{rep}}(x, h)/E_{\text{rep}}(0, h)$  as a function of  $(r_0 - x)/r_0$  for different heights:  $h = 1.5r_0$  (line 1),  $h = r_0$  (line 2) and  $h = 0.5r_0$  (line 3). As is seen in figure 2(b), the equilibrium position of an atom at  $x = 0$  (point A) is unstable, whereas the equilibrium position of an atom at  $x = r_0$  (point B) is stable. Thus, atom will be displaced by a horizontal force to the position B above the cell center (in fact it should be displaced to the center of one of the three hexagonal cells around a position A).

We further suppose that the total interaction of H atom with C atom at a separation  $r$  below 1 nm is described by the Lennard–Jones interaction potential

$$U_{\text{LJ}}(r) = \frac{\alpha}{r^{12}} - \frac{\beta}{r^6}, \quad (10)$$

where  $\beta$  is the constant of interatomic van der Waals interaction. The equilibrium separation distance  $h_0$  between one C and one H atom satisfies the condition

$$-\left. \frac{\partial U_{\text{LJ}}(r)}{\partial r} \right|_{r=h_0} = \frac{12\alpha}{h_0^{13}} - \frac{6\beta}{h_0^7} = 0. \quad (11)$$

This leads to the relation  $\beta = 2\alpha/h_0^6$ .

The total force acting on an H atom at a height  $h$  in the position B is determined by the six neighboring C atoms. It is equal to the sum of vertical projections of forces with potential (10)

$$F_B = \frac{72\alpha h}{(r_0^2 + h^2)^7} - \frac{36\beta h}{(r_0^2 + h^2)^4}. \quad (12)$$

The hydrogen atom would be absorbed by a nanotube if  $F_B < 0$  for any value of  $h$ . Taking into account the above connection between  $\alpha$  and  $\beta$ , we obtain from (12)

$$\frac{1}{(r_0^2 + h^2)^3} - \frac{1}{h_0^6} < 0. \quad (13)$$

This inequality is for sure satisfied if  $h_0 < r_0$ .

It is common knowledge [30, 31] that the equilibrium position of the two atoms

$$h_0 \approx R_{\text{ion}}^{(1)} + R_{\text{ion}}^{(2)} \leq R_a^{(1)} + R_a^{(2)}, \quad (14)$$

where  $R_{\text{ion}}^{(k)}$  and  $R_a^{(k)}$  are the so-called *ionic* and *atomic* radii, respectively. For C and H atoms under consideration it holds  $R_a^{(C)} = 0.77 \text{ \AA}$  and  $R_a^{(H)} = 0.53 \text{ \AA}$  [32]. Thus, in our case

$$h_0 \leq R_a^{(C)} + R_a^{(H)} = 1.3 \text{ \AA}. \quad (15)$$

If to take into account that for graphite cell  $r_0 = 1.42 \text{ \AA}$ , we arrive at the conclusion that the condition  $h_0 < r_0$  is satisfied and hydrogen atom will be absorbed by a nanotube.

#### 4. Conclusions and discussion

In the above we have presented the Lifshitz-type formulae for the van der Waals and Casimir free energy and force for the configuration of hydrogen atoms or molecules in close proximity to multi-walled or single-walled carbon nanotubes. Multi-walled nanotubes are approximately described by graphite dielectric permittivity, whereas single-walled nanotubes are considered in the approximation of a two-dimensional gas of free electrons. Both descriptions are of model character and do not claim complete description of all nanotube properties. They are applicable at separations larger than 1 nm. By comparing of calculation results for multi-walled nanotubes with those for single-walled nanotubes, the conclusion was made that the macroscopic description using the concept of dielectric permittivity is already applicable for nanotubes with only two or three walls depending on the separation distance to the hydrogen atom.

We have also considered separations below 1 nm where the exchange repulsion plays an important role. By disregarding the role of chemical forces, it was shown that under the influence of a lateral force originating from exchange repulsion, the hydrogen atom is moved toward a cell center. Simple analysis shows that at atomic distances above the cell center the exchange repulsion cannot balance the van der Waals attraction. As a result the hydrogen atom is absorbed by the nanotube. This is analogous to the effect of breaks on the constant force surfaces which arise when scanning of the monoatomic tip of an atomic force microscope above a surface in the strong repulsive mode. In future it would be interesting to consider the influence of the previously absorbed atoms on the absorption process and to determine the resulting absorption rate.

#### Acknowledgments

VMM and GLK are grateful to the Center of Theoretical Studies and Institute for Theoretical Physics, Leipzig University for their kind hospitality. They were supported by Deutsche Forschungsgemeinschaft, grant no 436 RUS 113/789/0-3.

#### References

- [1] Stivastava Y, Widom A and Friedman M H 1985 *Phys. Rev. Lett.* **55** 2246
- [2] Bordag M, Mohideen U and Mostepanenko V M 2001 *Phys. Rep.* **353** 1
- [3] Buks E and Roukes M L 2001 *Phys. Rev. B* **63** 033402
- [4] Chan H B, Aksyuk V A, Kleiman R N, Bishop D J and Capasso F 2001 *Science* **291** 1941  
Chan H B, Aksyuk V A, Kleiman R N, Bishop D J and Capasso F 2001 *Phys. Rev. Lett.* **87** 211801
- [5] Chumak A A, Milonni P W and Berman G P 2004 *Phys. Rev. B* **70** 085407
- [6] Kardar M and Golestanian R 1999 *Rev. Mod. Phys.* **71** 1233
- [7] Stipe B C, Mamin H J, Stowe T D, Kenny T W and Rugar D 2001 *Phys. Rev. Lett.* **87** 096801
- [8] Zurita-Sánchez J R, Greffet J-J and Novotny L 2004 *Phys. Rev. A* **69** 022902
- [9] Geyer B, Klimchitskaya G L and Mostepanenko V M 2005 *Phys. Rev. D* **72** 085009
- [10] Volokitin A I and Persson B N J 2007 *Rev. Mod. Phys.* **79** 1291
- [11] Hohenberg P and Kohn W 1964 *Phys. Rev.* **136** B864



- [12] Hult E, Hyldgaard P, Rossmeisl J and Lundqvist B I 2001 *Phys. Rev. B* **64** 195414
- [13] Bondarev I V and Lambin Ph 2005 *Phys. Rev. B* **72** 035451
- [14] Dobson J F, White A and Rubio A 2006 *Phys. Rev. Lett.* **96** 073201
- [15] Decca R S, López D, Fischbach E, Klimchitskaya G L, Krause D E and Mostepanenko V M 2007 *Phys. Rev. D* **75** 077101  
Decca R S, López D, Fischbach E, Klimchitskaya G L, Krause D E and Mostepanenko V M 2007 *Eur. Phys. J. C* **51** 963
- [16] Chen F, Klimchitskaya G L, Mostepanenko V M and Mohideen U 2007 *Opt. Express* **15** 4823  
Chen F, Klimchitskaya G L, Mostepanenko V M and Mohideen U 2007 *Phys. Rev. B* **75** 035338  
Chen F, Klimchitskaya G L, Mostepanenko V M and Mohideen U 2006 *Phys. Rev. Lett.* **97** 170402  
Klimchitskaya G L, Mohideen U and Mostepanenko V M 2007 *J. Phys. A: Math. Theor.* **40** F841
- [17] Blagov E V, Klimchitskaya G L and Mostepanenko V M 2005 *Phys. Rev. B* **71** 235401
- [18] Klimchitskaya G L, Blagov E V and Mostepanenko V M 2006 *J. Phys. A: Math. Gen.* **39** 6481
- [19] Lifshitz E M 1956 *Sov. Phys. JETP* **2** 73
- [20] Blocki J, Randrup J, Swiatecki W J and Tsang C F 1977 *Ann. Phys., NY* **105** 427
- [21] Barton G 2004 *J. Phys. A: Math. Gen.* **37** 1011  
Barton G 2005 *J. Phys. A: Math. Gen.* **38** 2997
- [22] Bordag M 2006 *J. Phys. A: Math. Gen.* **39** 6173
- [23] Bordag M, Geyer B, Klimchitskaya G L and Mostepanenko V M 2006 *Phys. Rev. B* **74** 205431
- [24] Blagov E V, Klimchitskaya G L and Mostepanenko V M 2007 *Phys. Rev. B* **75** 235413
- [25] Blagov E V, Klimchitskaya G L, Lobashov A A and Mostepanenko V M 1996 *Surf. Sci.* **349** 196
- [26] Blagov E V, Klimchitskaya G L and Mostepanenko V M 1998 *Surf. Sci.* **410** 158  
Blagov E V, Klimchitskaya G L and Mostepanenko V M 1999 *Tech. Phys.* **44** 970
- [27] Mazzitelli F D 2004 *Quantum Field Theory Under the Influence of External Conditions* ed K A Milton (Princeton: Rinton Press)
- [28] Palik E D (ed) 1985 *Handbook of Optical Constants of Solids* (New York: Academic)
- [29] Caride A O, Klimchitskaya G L, Mostepanenko V M and Zanette S I 2005 *Phys. Rev. A* **71** 042901
- [30] Israelachvili J 1992 *Intermolecular and Surface Forces* (New York: Academic)
- [31] Torrens I M 1972 *Interatomic Potentials* (New York: Academic)
- [32] Kittel C 1996 *Introduction to Solid State Physics* (New York: Wiley)